Solvent assisted formation of ruthenium(III) and ruthenium(II) hydrazone complexes in one-pot with potential *in vitro* cytotoxicity and enhanced LDH, NO and ROS release

Eswaran Jayanthi,[a] Sivalingam Kalaiselvi,[b] Viswanatha Vijaya Padma, [b] Nattamai S.P.Bhuvanesh,[c] Nallasamy Dharmaraj [a]

[a]Inorganic & Nanomaterials Research Laboratory, Department of Chemistry, Bharathiar University, Coimbatore – 641 046, India. E-mail: dharmaraj@buc.edu.in;

Tel.: +91 422 2428319; Fax: +91 422 2422387.

[b]Department of Biotechnology, Bharathiar University, Coimbatore 641 046, India.

[c]Department of Chemistry, Texas A&M University, College Station, TX 77843, U.S.A.

Electronic Supplementary Information

Mass spectra of all the four complexes (Fig. S1 - S4†), electronic spectra of complexes **3** and **4** in Tris-HCl buffer upon addition of CT-DNA (Fig. S5† and S6†), $[DNA]/[\varepsilon_a-\varepsilon_f]$ versus [DNA] plot (Fig. S7†), Stern-Volmer plot (Fig. S8†), emission spectra of BSA (1 μM) in the presence of increasing amounts of complexes **1**, **2**, **3**, and **4** (0−12 μM) (Fig. S9†), absorption titration of complexes with BSA (Fig. S10†) and synchronous spectra of BSA (1 μM) in the presence of increasing amounts of complexes **1**, **2**, **3**, and **4** (0−12 μM) in the wavelength difference of $\Delta\lambda$ = 15 nm and $\Delta\lambda$ = 60 nm (Fig.S11† and S12†). This material is available free of charge via the Internet at http://pubs.acs.org. Crystallographic data for the structures reported in this paper have been deposited with the Cambridge Crystallographic Data Centre (CCDC) as supplementary publication numbers CCDC-897084, 897083, 897086 and 932058 for the ruthenium complexes **1**−**4**. Copies of the data can be obtained free of charge from the CCDC (12 Union Road, Cambridge CB2 1EZ, U.K.; Tel: +44−1223−336408; Fax: +44−1223−336003; Email: deposit@ccdc.cam.ac.uk; Web site: http://www.ccdc.cam.ac.uk).

Fig. S1 ESI-MS spectrum of complex **1**

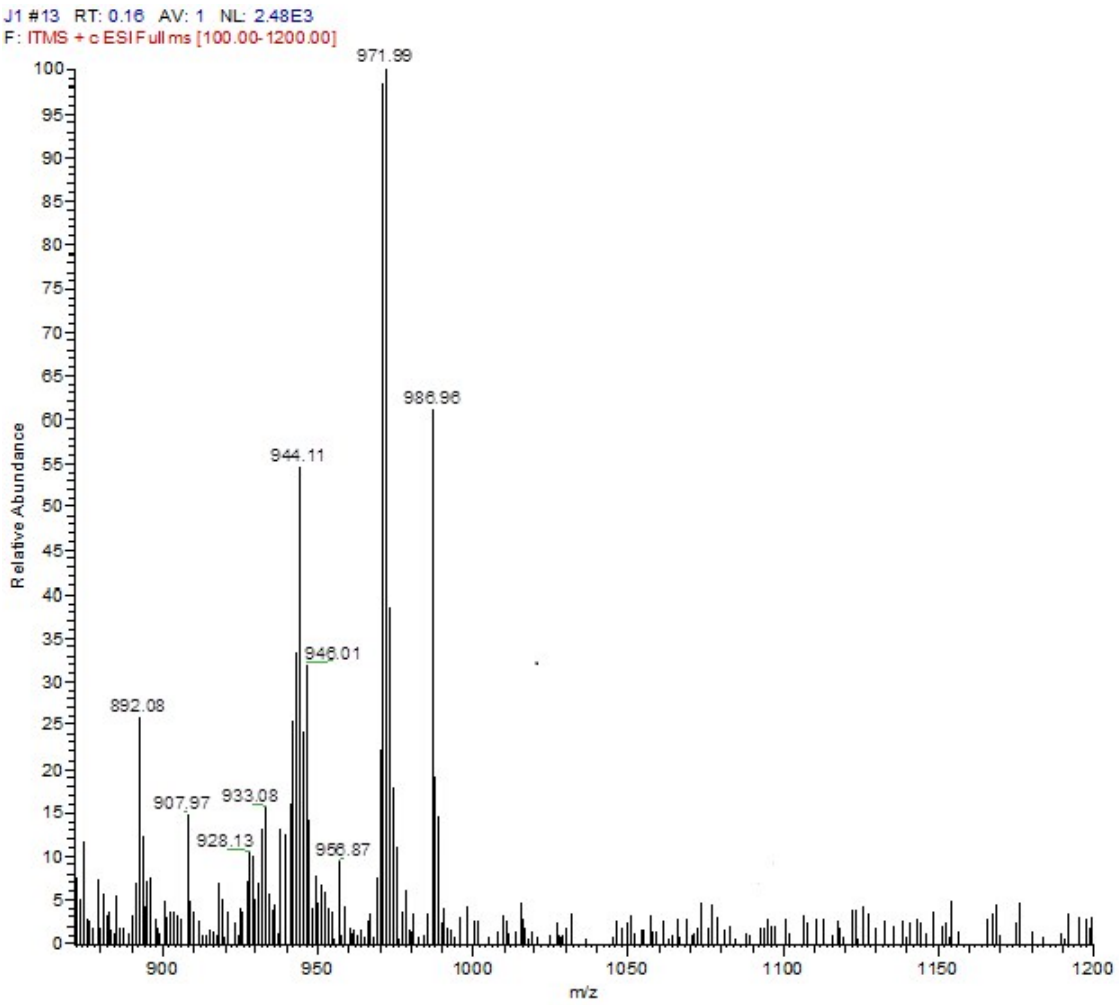

Fig. S2 ESI-MS spectrum of complex **2**

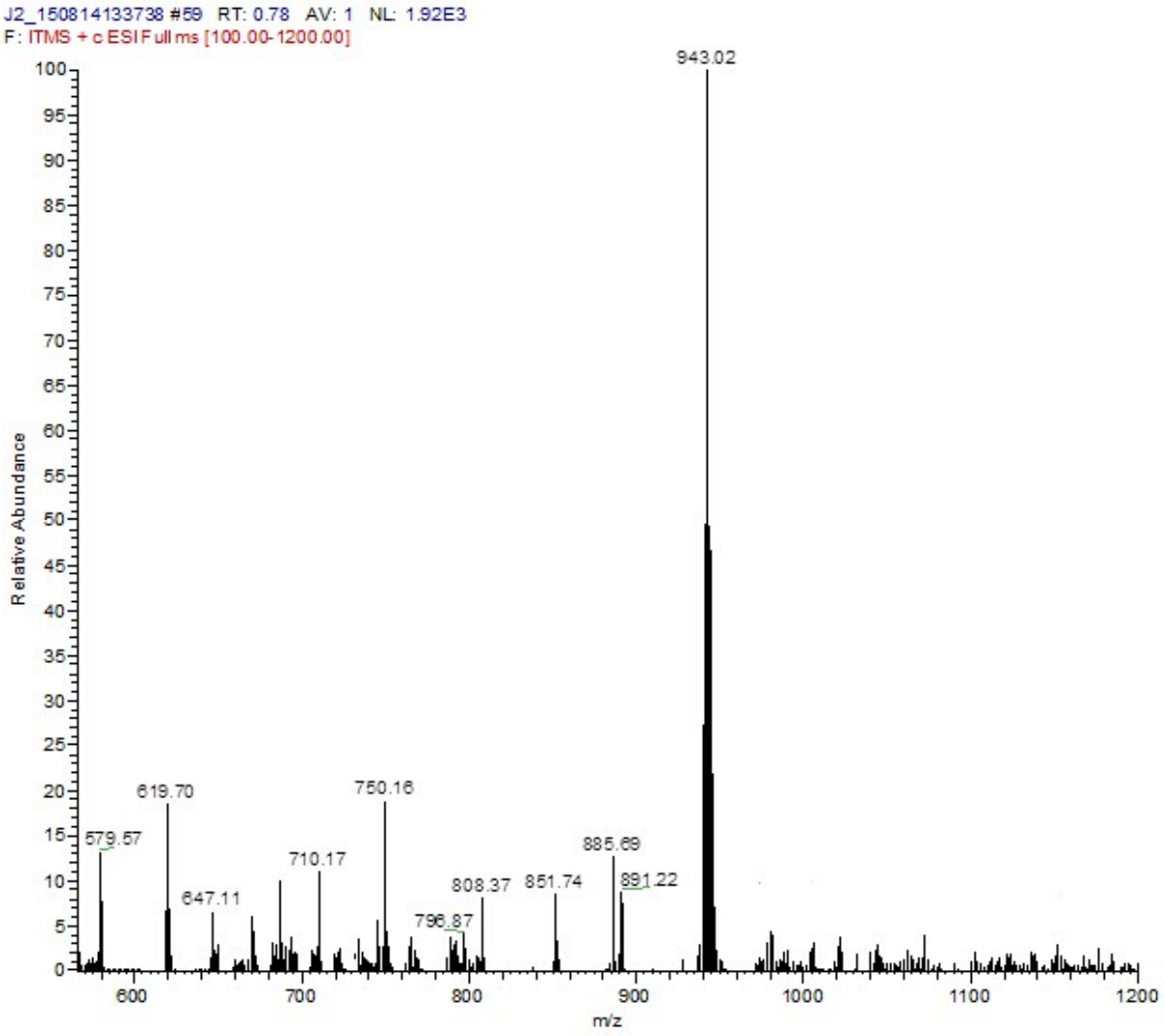

Fig. S3 ESI-MS spectrum of complex **3**

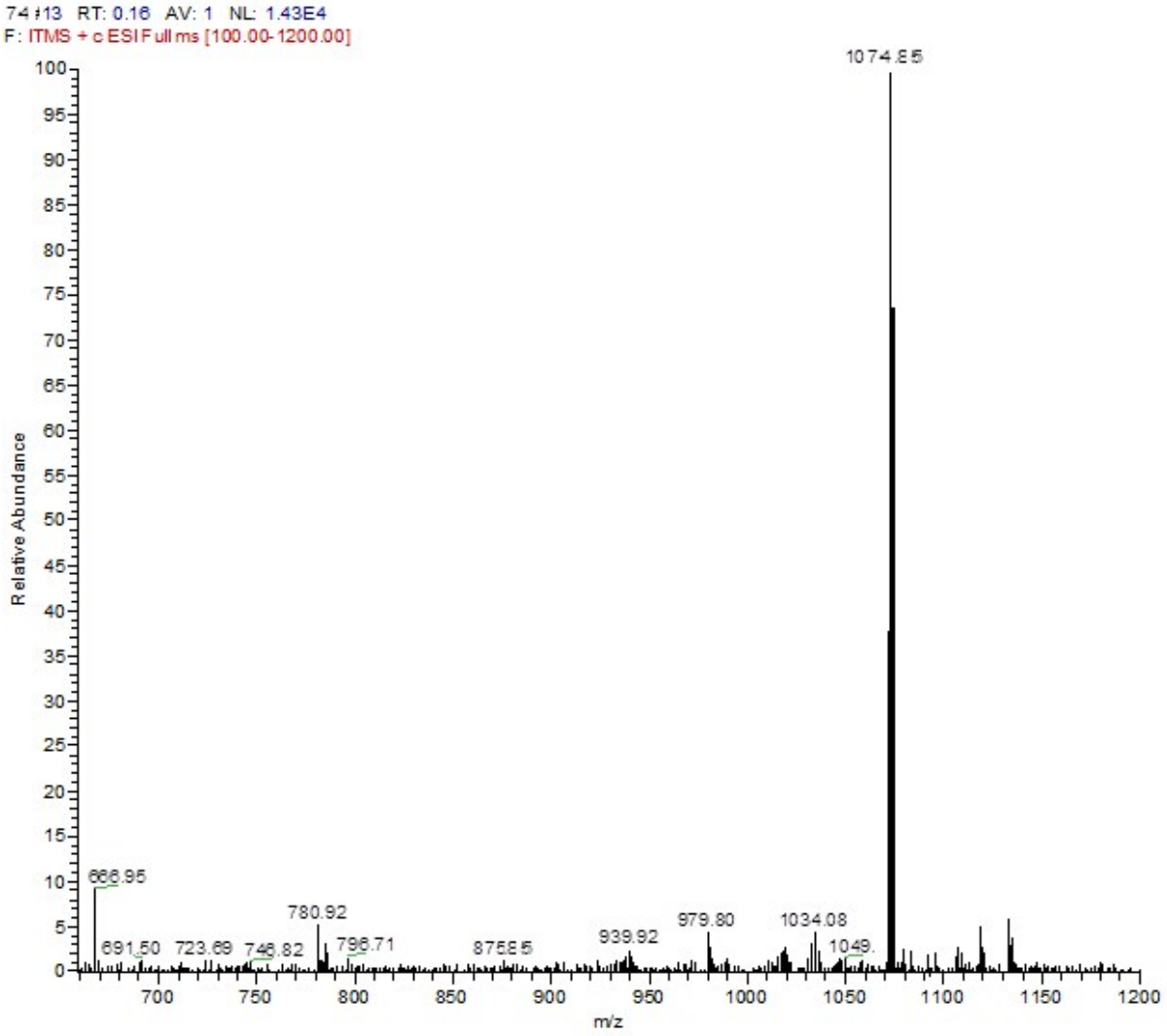

Fig. S4 ESI-MS spectrum of complex **4**

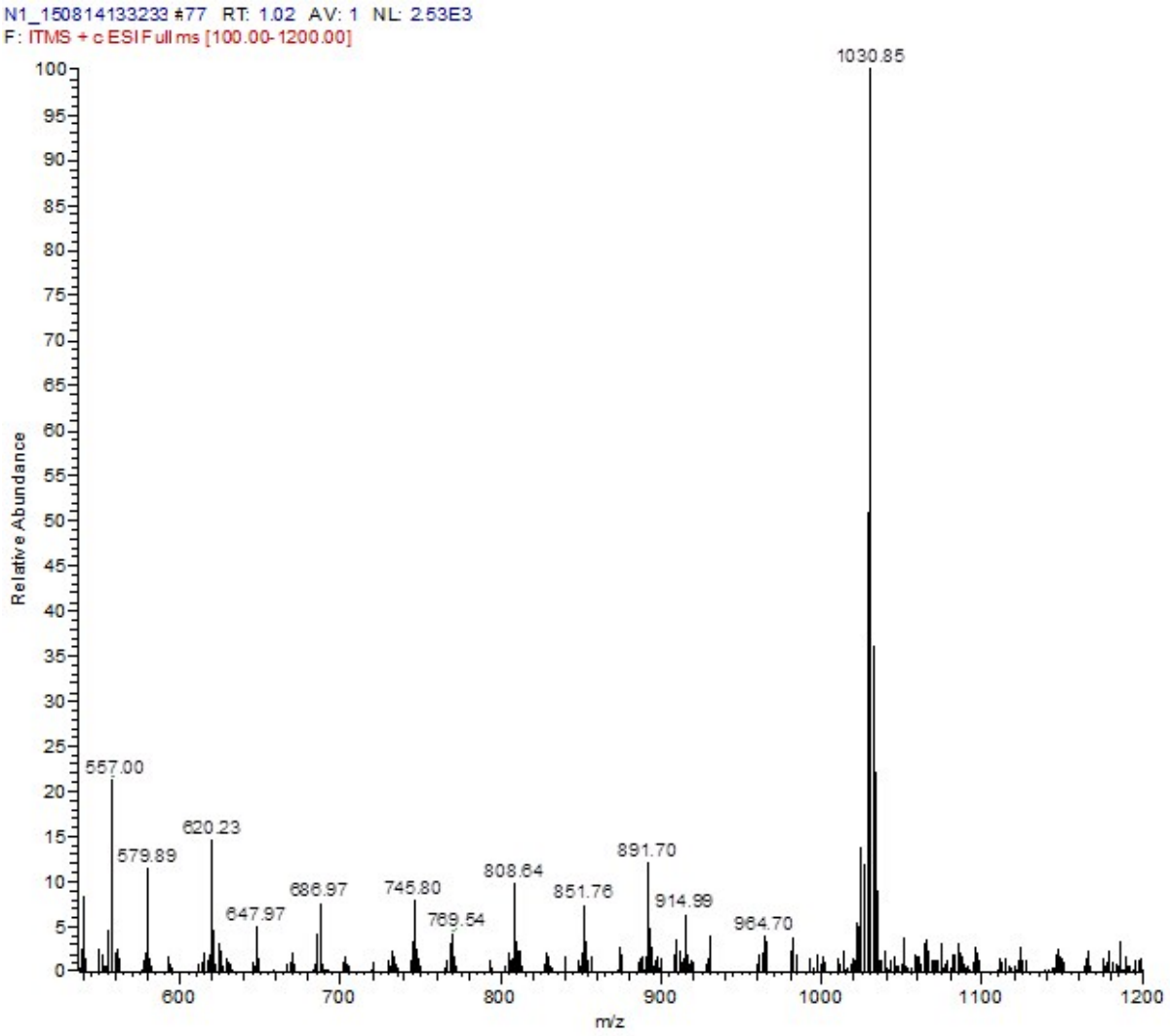

Fig. S5 Electronic spectra of complex **3** in Tris-HCl buffer upon the addition of CT-DNA. [Complex] = 25 μM, [DNA] = 0−20 μM. Arrow shows that the absorption intensities decrease upon increasing DNA concentration

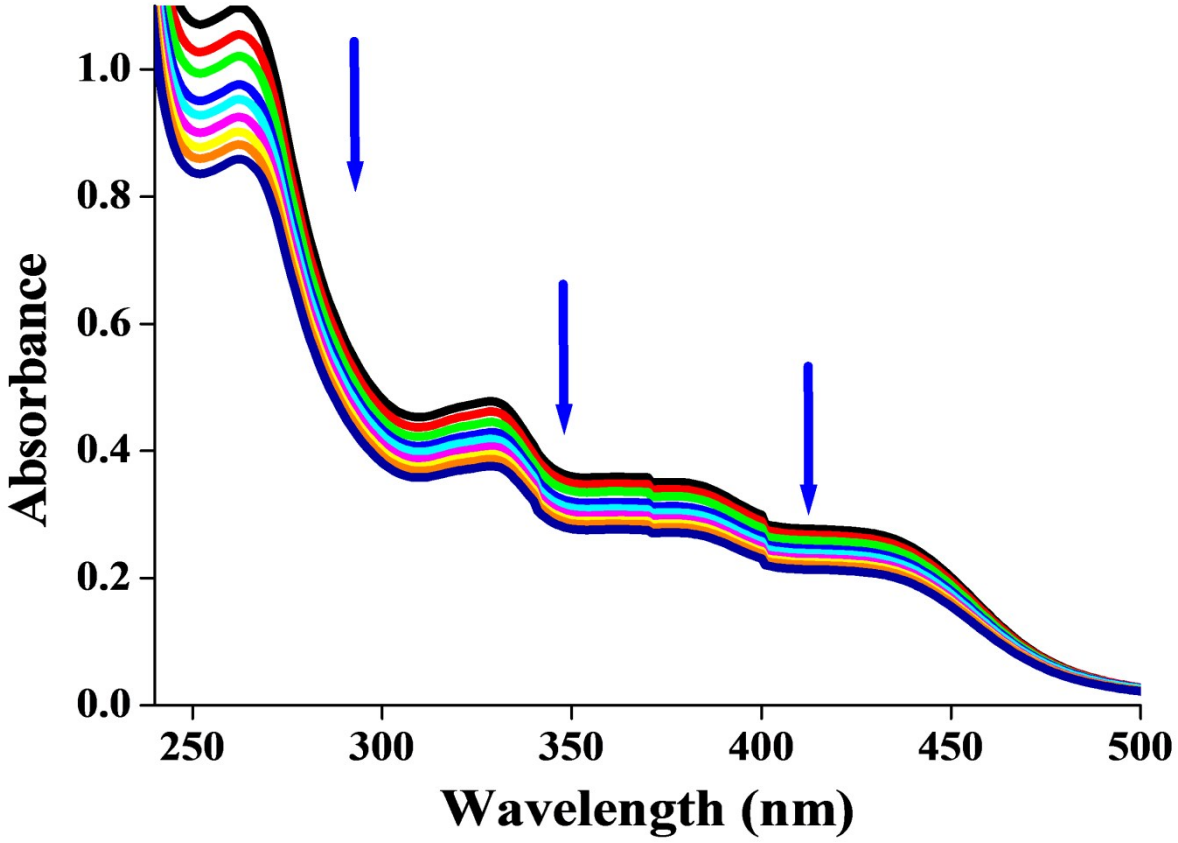

Fig. S6 Electronic spectra of complexes **4** in Tris-HCl buffer upon addition of CT-DNA. [Complex] = 25 μM, [DNA] = 0−20 μM. Arrow shows that the absorption intensities decrease upon increasing DNA concentration

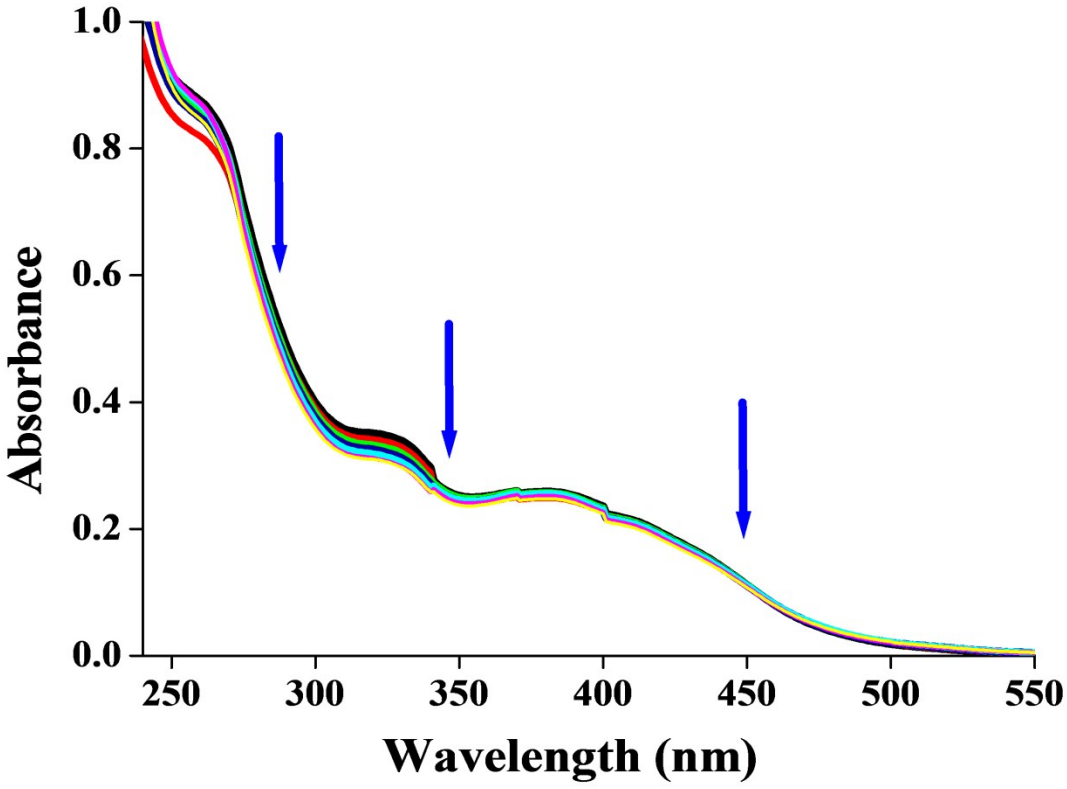

Fig. S7 Plots of [DNA]/($\varepsilon_a - \varepsilon_f$) versus [DNA] for complexes **1**-**4** with CT-DNA

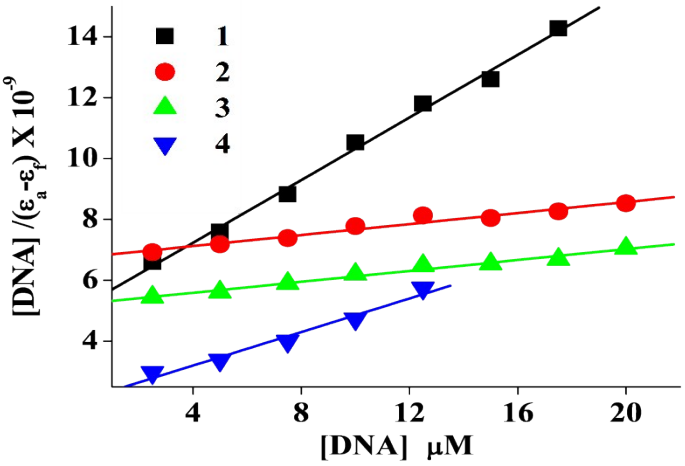

Fig. S8 Stern−Volmer plots of the EB−DNA fluorescence titration for complexes **1 - 4**.

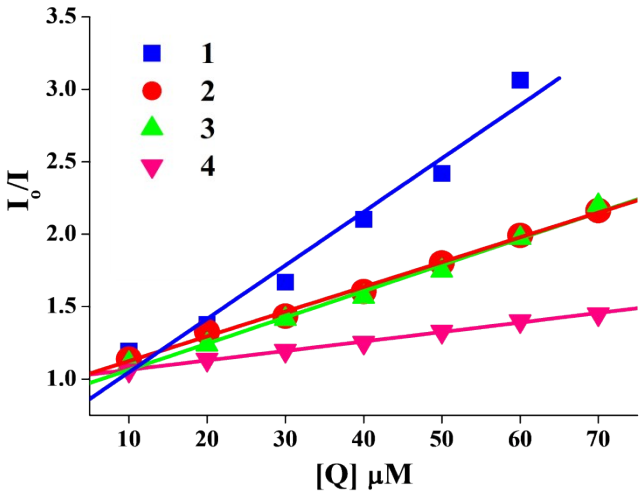

Fig.S9 Emission spectrum of BSA (1 μM; λexi = 280 nm; λemi = 346 nm) in the presence of increasing amounts of complexes **1 - 4** (0−12 μM). Arrow shows that the emission intensity changes upon increasing complex concentration.

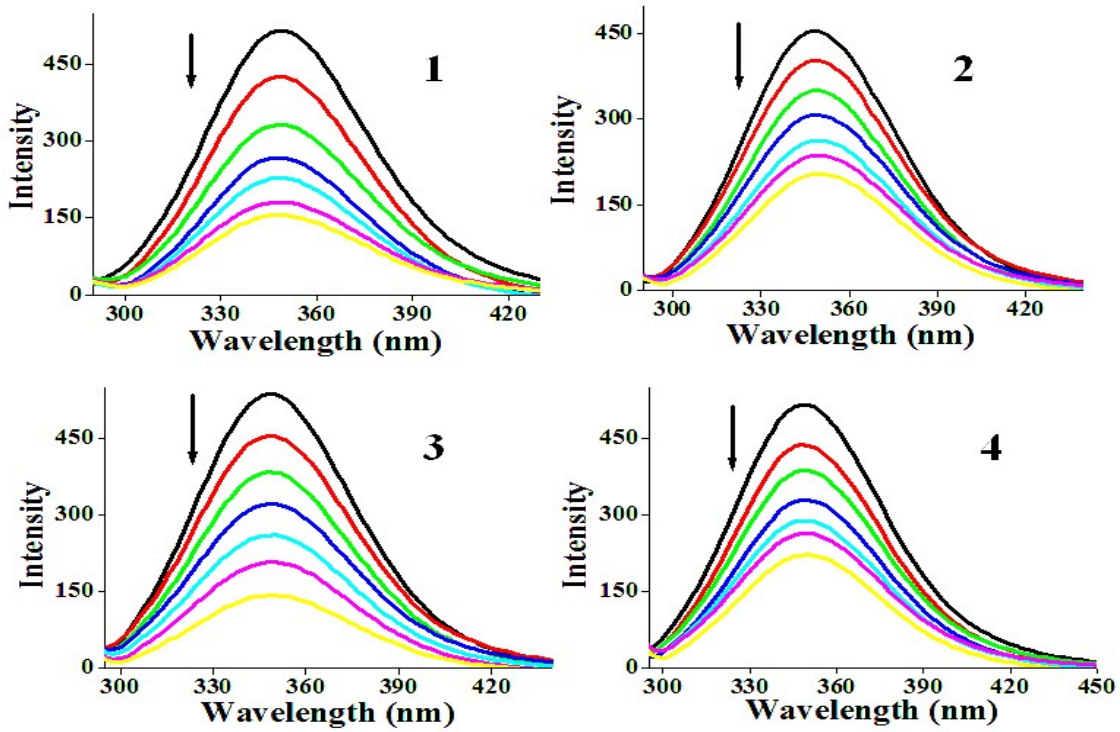

Fig.S10 UV absorption spectra of BSA (10 μM) in the presence of complexes **1 - 4** (0 and 5 μM).

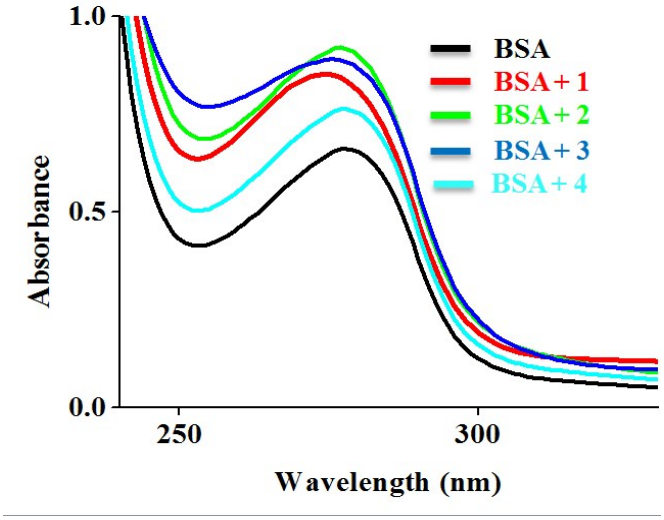

Fig. S11 Synchronous spectra of BSA (1×10^{-6} M) as a function of concentration of the complex (0-10 μM) with wavelength difference of $\Delta\lambda$= 15 nm), Arrow indicates the change in emission intensity with respect to concentration of complexes **1- 4**.

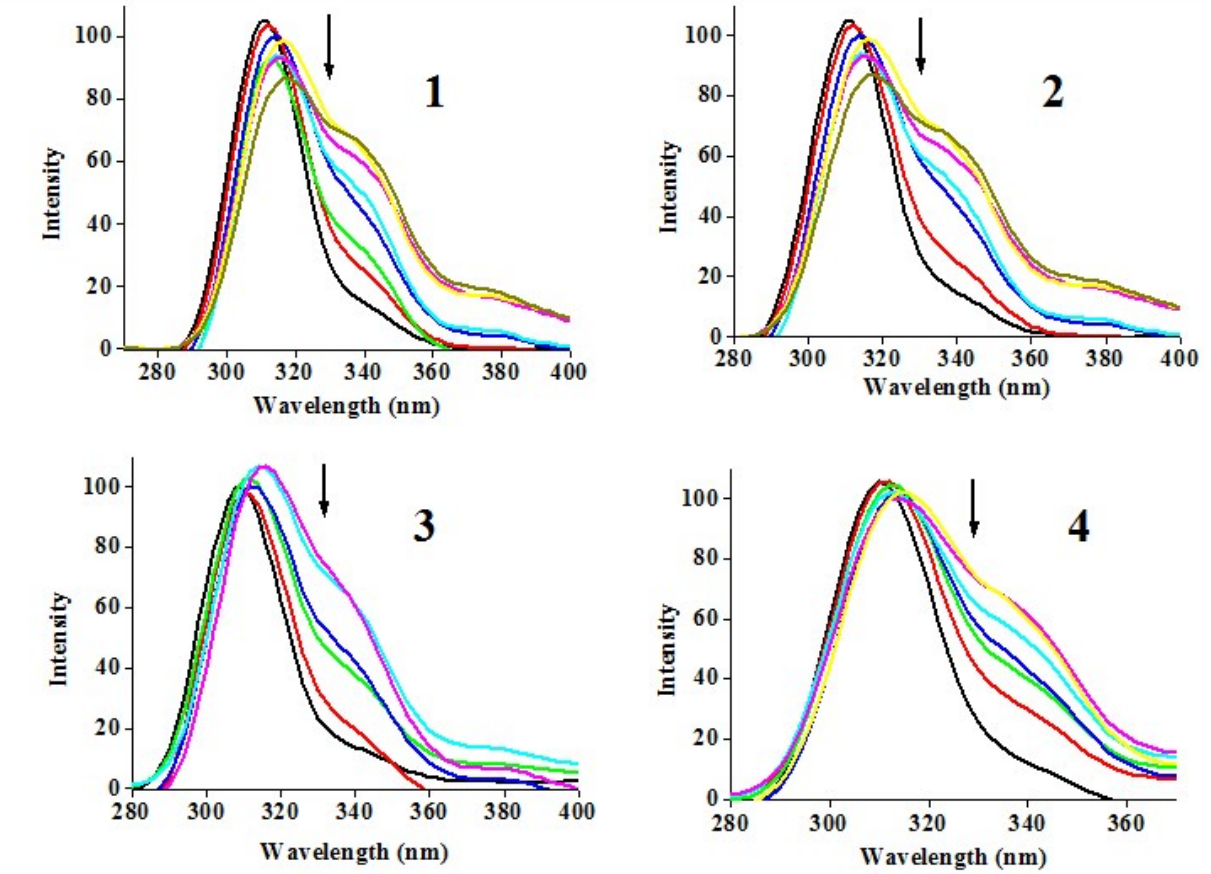

Fig. S12 Synchronous spectra of BSA (1×10^{-6} M) as a function of concentration of the complex (0-10 μM) with wavelength difference of $\Delta\lambda$=60 nm), Arrow indicates the change in emission intensity with respect to concentration of complexes **1- 4**.